Journal of Molecular Catalysis A: Chemical 309 (2009) 28–34

Contents lists available at ScienceDirect

Journal of Molecular Catalysis A: Chemical

journal homepage: www.elsevier.com/locate/molcata

Surface and catalytic properties of V_2O_5–TiO_2/SO_4^{2-} catalysts for the oxidation of methanol prepared by various methods

H. Zhao [a,b], S. Bennici [a], J. Shen [b], A. Auroux [a,*]

[a] Université Lyon 1, CNRS, UMR 5256, Institut de recherches sur la catalyse et l'environnement de Lyon (IRCELYON), 2 avenue Albert Einstein, F-69626 Villeurbanne, France
[b] Laboratory of Mesoscopic Chemistry, School of Chemistry and Chemical Engineering, Nanjing University, Nanjing 210093, China

ARTICLE INFO

Article history:
Received 19 January 2009
Received in revised form 21 April 2009
Accepted 21 April 2009
Available online 3 May 2009

Keywords:
V_2O_5–TiO_2/SO_4^{2-}
Adsorption microcalorimetry
Acidity
Methanol selective oxidation
Dimethoxymethane

ABSTRACT

The influence of the preparation method on the surface and catalytic properties of sulfated vanadia–titania catalysts has been studied. V_2O_5–TiO_2/SO_4^{2-} (VTiS) catalysts with 25 wt% V_2O_5 and 0.2–6.5 wt% S were prepared by co-precipitation, sol–gel and mechanical grinding methods and calcined at 723 K in air. The structural properties were characterized by O_2 chemisorption and laser Raman spectroscopy (LRS). The surface acidity was determined by the techniques of NH_3 adsorption microcalorimetry and pyridine adsorption infrared spectroscopy (FT-IR). Catalytic tests of oxidation of methanol to dimethoxymethane (DMM) were performed at atmospheric pressure in a fixed-bed micro-reactor. The Raman spectra revealed that vanadia existed in the form of a crystalline V_2O_5 phase. The results of ammonia adsorption of microcalorimetry showed a much lower heat of adsorption for samples with high content of SO_4^{2-}. Meanwhile, pyridine adsorption of FT-IR showed that both Lewis and Brønsted acid sites were present on the surface of all VTiS catalysts. The catalytic performance was also influenced by the preparation methods. VTiS-CP catalyst, prepared by co-precipitation, exhibited the highest DMM yield with a DMM selectivity of 86% for 61% methanol conversion at 423 K.

1. Introduction

During the last 20 years, numerous papers [1–7] have been devoted to the development of selective catalysts for the partial oxidation of methanol, with important industrial applications as a target. V_2O_5–TiO_2 (VTi) catalysts are recognized as suitable systems for the partial oxidation of methanol [1–3], and recent publications [4,5] show that the selective oxidation of methanol to dimethoxymethane (DMM) over V_2O_5–TiO_2 catalysts can be improved by doping VTi catalysts with SO_4^{2-} ions. In the reaction of methanol oxidation, DMM has usually been regarded as a by-product and has not been extensively studied. DMM has an extremely low toxicity and can be used as an excellent solvent in pharmaceutical and perfume industries, as a reagent in organic synthesis [8], and as an intermediate for the production of concentrated formaldehyde [9]. Importantly, it has been also recently reported that DMM can be effectively steam-reformed to produce H_2 for fuel cells [10]. Generally DMM is produced by condensation of formaldehyde with methanol over acidic catalysts [11]. Furthermore, methanol is one of the most important chemical intermediates used in the chemical industry, and the oxidation of methanol has been widely used as a probe reaction to characterize the activity of oxide catalysts [12–14] interpreted in terms of both structural and chemical (acidic and redox) properties.

It is well known that the acidity of solid catalysts is an important factor that determines their applications as industrial catalysts, and, consequently, many of their catalytic properties can be directly related to their acidity [15]. Adsorption microcalorimetry can be used to determine the distribution of heats of adsorption as well as the "acidity spectrum" of a catalyst surface. Previous results in the literature [15,16] have also shown that heats of ammonia adsorption can be taken into account for characterizing the surface of acid catalysts and correlated with their activity and selectivity in a variety of reactions. This motivated the use of ammonia adsorption microcalorimetry and pyridine adsorption FT-IR in conjunction with catalytic performance tests to investigate the influence of the preparation method on the surface and catalytic properties of V_2O_5–TiO_2/SO_4^{2-} catalysts.

The surface structure and vanadium dispersion were studied by Raman spectroscopy and O_2 chemisorption, respectively. Ammonia adsorption calorimetry was used to determine the number and strength of the surface acid sites of the V_2O_5–TiO_2/SO_4^{2-} (VTiS) catalysts, while the nature of the acid sites present on the catalysts was determined by pyridine adsorption FT-IR. The catalytic reaction of selective oxidation of methanol to DMM over V_2O_5–TiO_2/SO_4^{2-} catalysts was tested and the results analyzed in relation with the preparation methods.

* Corresponding author. Fax: +33 472445399.
E-mail address: aline.auroux@ircelyon.univ-lyon1.fr (A. Auroux).

1381-1169/$ – see front matter © 2009 Elsevier B.V. All rights reserved.
doi:10.1016/j.molcata.2009.04.011

2. Experimental

2.1. Catalyst preparation

In this work, four samples with the same theoretical amount of vanadia loading (25 wt%) were prepared by using different procedures, namely co-precipitation (sample VTiS-CP), co-precipitation with 1% polyethylene glycol (VTiS-CPEG), sol–gel (VTiS-SG) and mechanical grinding (VTiS-MG). The precursors were respectively $VOSO_4$ and $TiOSO_4$ for VTiS-CP and VTiS-CPEG, vanadyl acetylacetonate and titanium isopropoxide plus sulfuric acid for VTiS-SG, TiO_2 and $VOSO_4$ for VTiS-MG. The samples were all calcined at 723 K in air for 5 h, except sample VTiS-SG for which the calcination time was increased up to 12 h for a better decomposition of the precursors.

The details of the preparation methods have been previously described in [17].

2.2. Catalyst characterization

Raman spectroscopy measurements were performed using a LabRAM HR (Jobin Yvon) spectrometer. The excitation was provided by the 514.5 nm line of an Ar^+ ion laser (Spectra Physics) employing a laser power of 100 μW. The laser beam was focused through microscope objective lenses (100×) down to a 1 μm spot on the sample.

The dispersion of the vanadium species was measured on a Micromeritics 2010 apparatus by using the high temperature oxygen chemisorption (HTOC) method [18]. The samples were reduced in purified H_2 flow (154 mL min^{-1}) at 640 K for 2 h followed by evacuation at the same temperature for 4 h, and then oxygen uptake was measured at the same temperature.

The pyridine adsorption infrared spectra were recorded with a Bruker Vector 22 FT-IR spectrophotometer (DTGS detector), in the 4000–400 cm^{-1} range, with a resolution of 2 cm^{-1} and using 100 scans. The self-supporting wafer (10–30 mg, 18 mm diameter) was first activated in situ at 573 K in oxygen flow for 14 h, then evacuated at the same temperature for 2 h and then exposed to pyridine (Air Liquide, 99.8%, vapor pressure 3.3 kPa) at room temperature for 5 min. The desorption was carried out by evacuation for 30 min each at room temperature, 373 K, 473 K and 573 K. The spectra were recorded at room temperature after adsorption and desorption at each temperature.

The microcalorimetric studies of ammonia adsorption were performed at 423 K in a heat flow calorimeter (C80 from Setaram) linked to a conventional volumetric apparatus equipped with a Barocel capacitance manometer for pressure measurements. The ammonia used for the measurements (Air Liquide, purity >99.9%) was purified by successive freeze–pump–thaw cycles. About 100 mg of sample was pretreated in a quartz cell under evacuation overnight at 623 K. The differential heats of adsorption were measured as a function of coverage by repeatedly introducing small doses of ammonia gas onto the catalyst until an equilibrium pressure of about 66 Pa was reached. The sample was then outgassed for 30 min at the same temperature, and a second adsorption was performed at 423 K until an equilibrium pressure of about 27 Pa was attained in order to calculate the irreversibly chemisorbed amount of ammonia at this pressure.

2.3. Catalytic reaction

The oxidation of methanol was carried out in a fixed-bed microreactor made of glass with an inner diameter of 6 mm. The methanol was introduced into the reaction zone by bubbling O_2/N_2 (1/5) through a glass saturator filled with methanol (99.9%) maintained at 278 K. In each test, 0.2 g of catalyst was loaded, and the gas hourly space velocity (GHSV) was 11,400 ml g^{-1} h^{-1}. The feed composition was kept constant at methanol:O_2:N_2 = 1:3:15 (v/v). The tail gas out of the reactor was analyzed by an on-line GC equipped with an FID detector and a TCD detector. The column used was PORAPAK N for the separation of methanol, DMM and other organic compounds. The gas lines were kept at 373 K to prevent condensation of the reactant and products. The reaction was carried out at atmospheric pressure.

3. Results and discussion

The samples are listed in Table 1 together with their surface areas and chemical compositions. As can be seen, the vanadia loadings were close to the theoretical one (25 wt%) but the sulfur amount varied greatly with the preparation method.

3.1. Surface structures

Oxygen adsorption can be used to evaluate the dispersion of a metal oxide on the surface of a support. Parekh and Weller [19,20] proposed a low temperature oxygen chemisorption (LTOC) method while Oyama et al. [18] suggested a HTOC method. Prereducing the samples at the same temperature as that used to measure oxygen uptakes (640 K) seems to prevent bulk reduction and leads to more reliable dispersion values [18,21]. Therefore, this method was adopted for the measurements of vanadium dispersion in this work.

The surface oxygen atom densities were calculated starting from the oxygen uptakes (determined by O_2 chemisorption) and the BET surface areas (determined by N_2 adsorption at 77 K), and are reported in Table 1. The total number of vanadium sites on each sample (expressed as the number of V atoms per unit surface area) was calculated starting from the metal content determined by chemical analysis and is also reported as comparison in Table 1. Wachs et al. reported that the theoretical density for the monolayer dispersion of vanadia on TiO_2 is 7.9×10^{18} V m^{-2} [22]. From the total vanadium loadings presented in Table 1 it can be noticed that all samples display loadings higher than the monolayer capacity, thus confirming the existence of a crystalline V_2O_5 phase in our samples as determined by Raman analysis (see next paragraph) and XRD [17].

The oxygen site density values were 8.6×10^{18}, 17.6×10^{18}, 24.1×10^{18} and 3.2×10^{18} m^{-2} for VTiS-CP, VTiS-CPEG, VTiS-SG and VTiS-MG, respectively.

Unfortunately, the oxygen atom site densities were higher than the average density of V=O groups on the low-index planes of V_2O_5 (5.0×10^{18} atom m^{-2}) [18], indicating that the HTOC technique did titrate some bulk V_2O_5, making it impossible to calculate the real dispersion of vanadium. Indeed, this technique is better suited for the study of samples prepared by impregnation or atomic layer deposition. However, the determination of the oxygen site density makes it possible to compare the surface properties of the different samples independently of their specific surface area.

The surface structure of vanadia and titania species on the VTiS catalysts was examined by Raman spectroscopy, from 1600 to 200 cm^{-1}, as shown in Fig. 1. It has been generally recognized that the Raman bands at 1030 and 900–100 cm^{-1} represent terminal V=O bonds in monomeric vanadyl and polymeric vanadate species, respectively [23–25]. Crystalline V_2O_5 displays Raman bands around 996, 703, 530, 483, 406, 306 and 285 cm^{-1} [26,27]. It is important to note that there were some yellow particles among the white particles of sample VTiS-MG; thus, the VTiS-MG catalyst is not homogeneous, and consequently both types of particles were analyzed. As can be seen in Fig. 1, all the catalysts exhibited typical Raman features of crystalline V_2O_5 with bands around 1002, 710, 535, 489, 412, 310 and 291 cm^{-1}. The formation of crystalline V_2O_5 on the catalyst surface has also been observed by XRD [17]. It can be

Table 1
Chemical analysis, BET surface areas, oxygen uptakes, and oxygen atom site density on the surface of V_2O_5–TiO_2/SO_4^{2-} catalysts.

Catalyst	CA (wt%)			S_{BET} ($m^2\,g^{-1}$)	O_2 uptake (mmol g^{-1})[a]	Total loading ($\times10^{18}$ V m^{-2})[b]	O site density ($\times10^{18}$ atom m^{-2})[c]
	V	Ti	S				
VTiS-CP	13.4	43.8	0.2	105	0.75	15.1	8.6
VTiS-CPEG	13.4	45.1	0.2	74	1.08	21.4	17.6
VTiS-SG	11.4	44.8	1.4	43	0.86	31.3	24.1
VTiS-MG	12.4	34.6	6.5	132	0.35	11.1	3.2

[a] Reduction of samples by H_2 and O_2 adsorption were both performed at 640 K.
[b] Supposing that all the vanadium atoms are located on the surface.
[c] Supposing that each surface V adsorbs an oxygen atom.

also seen that strong Raman bands due to the covalent character of Ti–O bonds [22] appeared at 650, 528 and 408 cm^{-1} for all the VTiS catalysts except for VTiS-MG-yellow particles, suggesting that these yellow particles were mostly composed of vanadia. It was reported in the literature [28] that the sulfate species present on sulfated V_2O_5/TiO_2 samples display a characteristic band around 1370 cm^{-1} in the Raman spectra due to terminal S=O bonds. However, this band was not observed for our VTiS catalysts, even though surface sulfate species were detected by IR for the VTiS-MG catalyst [17].

3.2. Surface acidity

Ammonia adsorption microcalorimetry measurements were carried out to determine the number, strength and strength distribution of the surface acid sites of catalysts [15,29]. The results of the microcalorimetric measurements were used to complement the acidity study by FT-IR, and were correlated with the catalytic activity. The surface acidity was thus determined in terms of number of acid sites and sites strength. The results are presented in Figs. 2–4 and Table 2. Figs. 2 and 3 represent the differential heats and integral heats of NH_3 adsorption vs. coverage, respectively. As the samples displayed quite different surface areas (see Table 1) the adsorbed volumes have been expressed in μmol NH_3 per m^2 of catalyst.

The initial heats of ammonia adsorption observed on co-precipitated VTiS samples doped or not with 1 wt% PEG-400 were similar. The initial heats of NH_3 adsorption were 209 and 196 kJ mol^{-1} for the VTiS-CP and VTiS-CPEG samples, respectively (see Table 2), which indicates that these two samples are quite acidic, in agreement with the results from Hammett titration [30]. As can be seen in Fig. 2, low initial heats of adsorption were observed for the VTiS-SG and VTiS-MG samples, containing high content of sulfur. The low heat values recorded for the first four ammonia increments (which were totally consumed by the sample) were followed by an increase to higher heats of adsorption,

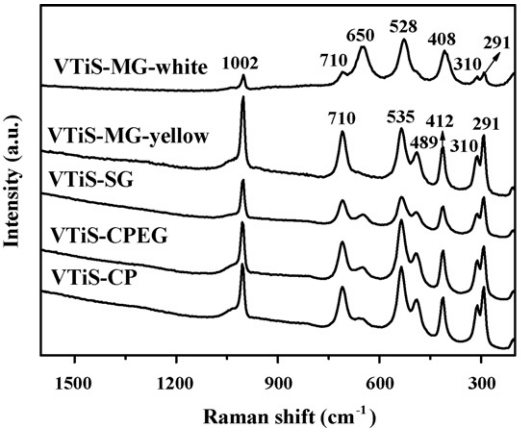

Fig. 1. Raman spectra of VTiS catalysts.

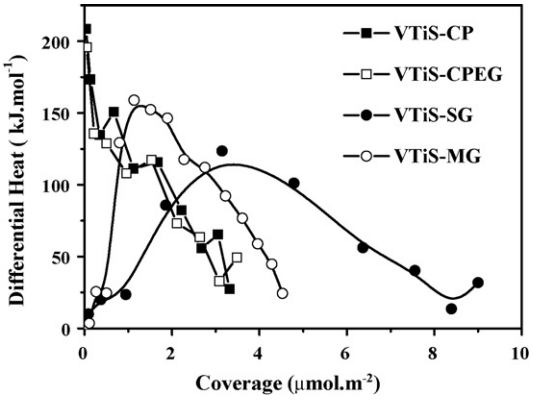

Fig. 2. Differential heat vs. coverage (in μmol m^{-2} of catalyst) for NH_3 adsorption at 423 K over VTiS catalysts.

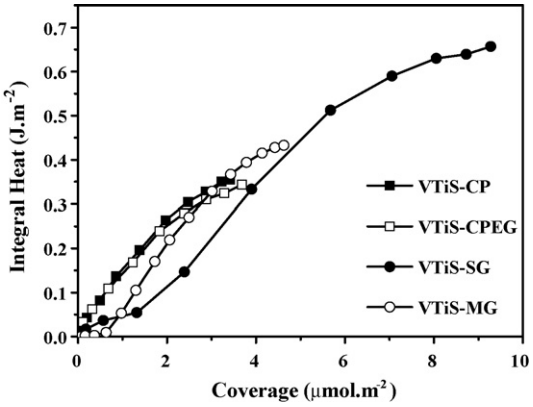

Fig. 3. Integral heat vs. coverage (in μmol m^{-2} of catalyst) for NH_3 adsorption at 423 K over VTiS catalysts.

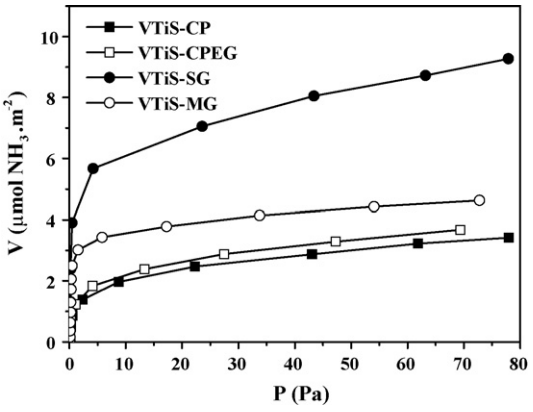

Fig. 4. Volumetric isotherms of NH_3 adsorption at 423 K for the VTiS catalysts.

Table 2
Total and irreversible adsorption of ammonia at a pressure of 27 Pa and an adsorption temperature of 423 K.

Sample	V_{tot}[a] (27 Pa) (μmol g^{-1})	V_{tot}[a] (27 Pa) (μmol m^{-2})	V_{irr}[b] (μmol g^{-1})	V_{irr}[b] (μmol m^{-2})	Q_{init}[c] (kJ mol^{-1})	Q_{int}[d] (27 Pa) (J g^{-1})
VTiS-CP	243	2.3	123	1.2	209	32
VTiS-CPEG	193	2.6	77	1.1	196	23
VTiS-SG	281	6.5	216	5.0	3	26
VTiS-MG	503	3.8	392	3.0	10	54

[a] Total amount of NH_3 retained as determined at 27 Pa of equilibrium pressure.
[b] "Irreversible" amount of NH_3 retained as determined from the difference between the amounts adsorbed in the first and second adsorptions at 27 Pa.
[c] Heat evolved from the first NH_3 dose.
[d] Total heat evolved at 27 Pa of NH_3 equilibrium pressure upon NH_3 adsorption.

corresponding to what is normally expected for a strong acid. This strange phenomenon can only be interpreted by the combination of two phenomena, endothermic and exothermic, respectively, thus inducing a lower initial heat. The very strong acid sites due to sulfate ions are supposed to create either a strong or dissociative chemisorption. It has been reported in the literature [16,31] that the first doses of NH_3 could dissociate at the surface (endothermic phenomenon) with the formation of OH species, evidenced by NH_3 adsorption infrared spectroscopy [31]. The lower heats of adsorption are then attributed to the contribution of NH_3 dissociation to the differential heat of adsorption. Another explanation could be the formation of ammonium sulfate (however this last possibility implies a transformation that is too exothermic [32], making it unlikely) or more probably ammonium sulfite. This particular behavior observed for samples containing a relatively high amount of sulfur made it difficult to appreciate the initial heats of adsorption of the sulfated oxides. As this phenomenon was scarcely observed by adsorption calorimetry for sulfated zirconias it is supposed to imply a special type of sulfur species on the catalyst surface, which could involve the support type and/or the preparation method. For co-precipitated catalysts with or without 1 wt% PEG-400, which contain a much lower amount of sulfur species, the heats of NH_3 adsorption gradually decreased with NH_3 coverage, revealing the heterogeneous strength distribution of these catalysts. Fig. 4, which represents the ammonia adsorption isotherms, did not reflect this particular behavior of samples VTiS-SG and VTiS-MG, thus confirming that these two samples are more acidic due to their higher sulfate species content.

As shown in Fig. 3, ammonia adsorption integral heat curves for VTiS-CP and VTiS-CPEG catalysts can be approximately viewed as sections of parabolas, and the highest parabola should correspond to the sample on which the titration of the largest amount of strong sites occurred [33]. The coverage being reported per unit of surface area (instead of g of catalyst) the two curves are very close and confirm the similar acidic behavior of the samples prepared by co-precipitation. The curves, for VTiS-SG and VTiS-MG samples, display a plateau in the low coverage region for the first four NH_3 doses, which can be associated to the strange phenomenon of very low initial differential heats of adsorption for these two samples. Therefore the parabolic sections of the curves are shifted to higher coverages.

The quantitative results of NH_3 adsorption are summarized in Table 2. The total amount of ammonia adsorbed at an equilibrium pressure of 27 Pa (V_{tot}) and the amount irreversibly adsorbed at the same pressure (V_{irr}) are indicative of the total number of acid sites on the surface of the sample and the amount of strong acid sites, respectively. Reported in μmol g^{-1}, both V_{tot} and V_{irr} varied in the order of VTiS-MG > VTiS-SG > VTiS-CP > VTiS-CPEG, greatly influenced by the preparation method and consequently by the sulfur amount. When V_{tot} and V_{irr} are expressed per unit surface area, the total and strong surface acid sites densities for the VTiS-CP and VTiS-CPEG samples are similar, while the VTiS-SG sample possesses more total and strong surface acid sites than VTiS-MG, which confirms the role played by the surface area in the determination of the acidity of solids (see Table 2 and Fig. 2). The data in Table 2 clearly indicate that most of the adsorbed ammonia is strongly chemisorbed on samples VTiS-SG and VTiS-MG, while the co-precipitated samples display a large part of physisorption.

IR spectroscopy of pyridine adsorption on supported vanadium oxide surfaces has been examined widely in the literature [34–37], as it can be used to distinguish between the different types of surface acid sites in the catalysts.

Fig. 5(A)–(D) present the IR spectra of pyridine adsorption on VTiS catalysts, after desorption at different temperatures: (a) 298 K, (b) 373 K, (c) 473 K, and (d) 573 K. All the spectra reported in Fig. 5 were obtained by subtracting the spectrum of the fresh catalyst (without pyridine adsorption at room temperature) from those obtained after pyridine adsorption. The same adsorption bands characteristic of pyridine on Lewis and Brønsted acid sites were observed for all VTiS catalysts, and no significant shift in the peak frequency positions was observed as a function of the preparation method. The bands at 1609, 1575, 1487 and 1448 cm^{-1} have been assigned to the 8a, 8b, 19a and 19b vibrational modes of pyridine coordinated to Lewis acid sites [34,36]. The bands at 1638 (v8a), 1575 (v8b), 1487 (v19a) and 1537 cm^{-1} (v19b) correspond to pyridinium ions bonded to Brønsted acid sites. The bands around 1487 (v19a) and 1575 cm^{-1} (v8b) are associated simultaneously to both Brønsted and Lewis acid sites. In addition to these peaks, at a desorption temperature of 298 K, the IR spectra of the catalysts show a peak at 1437 cm^{-1} corresponding to physisorbed pyridine. It has been reported in the literature [38] that pure V_2O_5 presents low Brønsted and Lewis acidities, while TiO_2 exhibits strong Brønsted and Lewis acidities according to the relative intensities of the bands around 1536 and 1446 cm^{-1}.

Two Lewis and Brønsted acid site peaks at ~1448 and 1537 cm^{-1}, respectively, were used to compare the acidity, i.e. the number and strength of the acid sites of the different catalysts. The absolute concentration of surface acid sites determined in this manner is subject to a ~10% error, as estimated in the literature [39,40]. However, reliable and valuable information can be obtained on a relative scale, when comparing the acidity in a series of catalysts [40].

Fig. 6 shows the integrated intensities of these two bands estimated by band-separation techniques of the spectra for VTiS catalysts. A quantitative comparison of the acid site populations of the samples can be performed by calculating the area under the LPy and BPy peaks [34,41,42]. Because of the possibility of physical re-adsorption on the surface with increasing evacuation temperatures, it is reasonable to compare the acid site populations at an evacuation temperature higher than 400 K. Therefore, the concentration of Brønsted and Lewis acid sites varied in the order of VTiS-MG > VTiS-CP > VTiS-CPEG > VTiS-SG, which indicates that the mechanical mixing sample which comes from the simple addition of titania and vanadyl sulfate is more acidic than the other samples, thus confirming the calorimetric results.

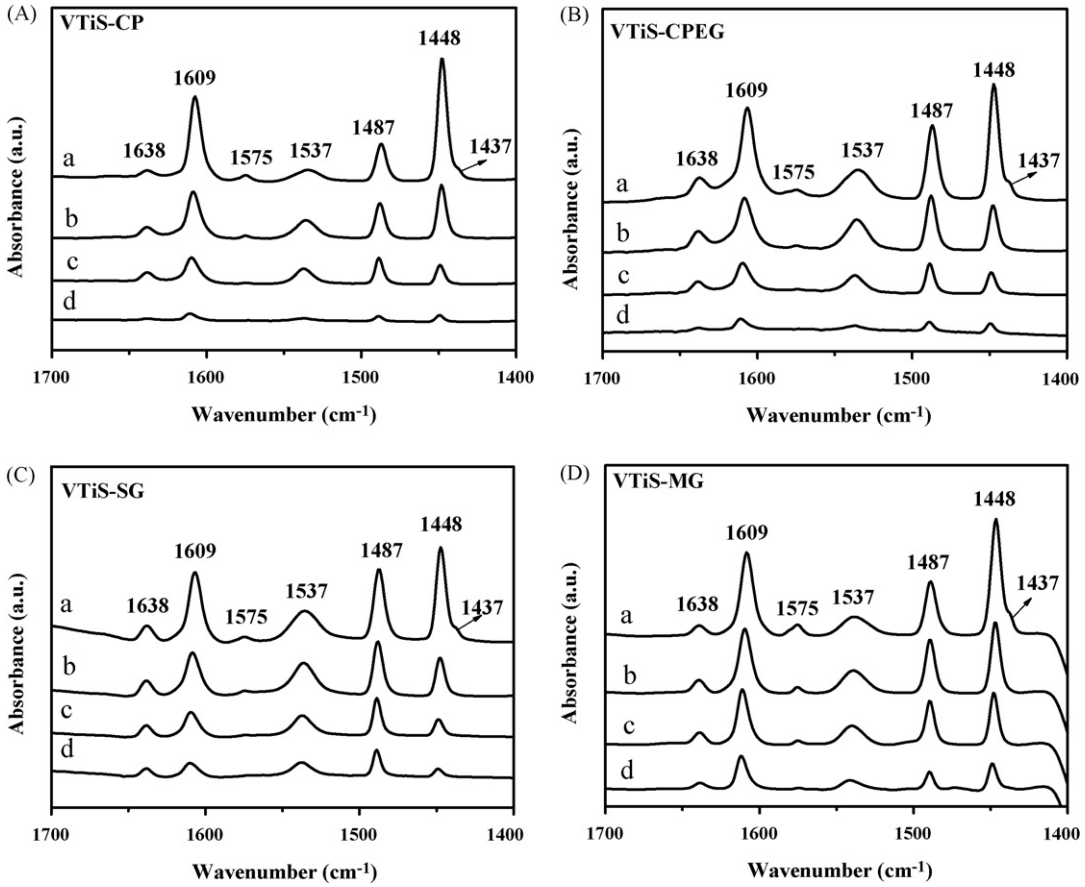

Fig. 5. FT-IR spectra for pyridine adsorption and desorption on (A) VTiS-CP, (B) VTiS-CPEG, (C) VTiS-SG and (D) VTiS-MG catalysts at different temperatures: (a) 298 K, (b) 373 K, (c) 473 K and (d) 573 K.

3.3. Methanol oxidation reaction

Methanol and its derivatives have been widely studied due to their industrial importance. In addition, the catalytic oxidation of methanol is a convenient structure-sensitive reaction. The distribution of products reflects the nature of the surface active sites: methanol is converted to formaldehyde (FA) and methyl formate (MF) on redox sites, to dimethyl ether (DME) on acidic sites, and to DMM on acidic and redox bi-functional sites [12,13]. Hence, the conversion of methanol can also be used to evaluate the surface acidic and redox properties of VTiS catalysts. The results are shown in Table 3 and Fig. 7.

The VTiS-CP catalyst, prepared by the co-precipitation method, showed the highest methanol conversion to DMM, but a drastic decrease in selectivity was observed for reaction temperatures higher than 423 K. In addition, the distribution of products on VTiS-

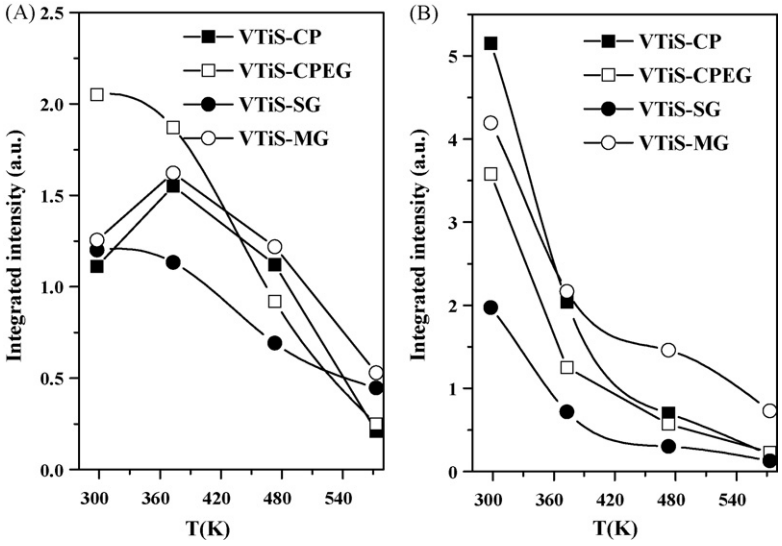

Fig. 6. Integrated intensity of BPy and LPy bands as a function of temperature on VTiS catalysts. (A) BPy band (1537 cm^{-1}); (B) LPy band (1448 cm^{-1}).

Table 3
Catalytic activities of the VTiS catalysts in the methanol oxidation reaction.

Sample	Temp. (K)	Methanol conversion (%)	Selectivity (%)				
			DMM	FA	MF	DME	CO_x
VTiS-CP	393	13	98	0	1	1	0
	403	24	96	0	3	1	0
	413	42	93	0	6	1	0
	423	61	86	1	12	1	0
	433	72	40	13	46	1	0
	443	87	1	6	74	2	17
VTiS-CPEG	393	10	98	0	1	1	0
	403	17	96	0	3	1	0
	413	23	83	9	7	1	0
	423	28	56	26	17	1	0
	433	37	24	38	37	1	0
	443	76	1	10	73	1	15
VTiS-SG	393	7	96	0	1	3	0
	403	12	97	0	2	1	0
	413	19	96	0	3	1	0
	423	33	93	0	6	1	0
	433	47	89	0	10	1	0
	443	65	72	2	25	1	0
VTiS-MG	393	2	93	0	0	7	0
	403	4	93	0	0	7	0
	413	8	91	2	0	7	0
	423	15	90	2	1	7	0
	433	21	88	3	1	8	0
	443	33	84	3	3	10	0

DMM: dimethoxymethane; FA: formaldehyde; MF: methyl formate; DME: dimethyl ether; CO_x: CO_2 (or CO).

CP catalyst indicates that the surface acidity was strong enough to catalyze the reaction of methanol to DMM, without producing a large amount of FA and MF as oxidation products (see Table 3). The catalytic performance of the VTiS-CPEG sample was similar to that of VTiS-CP, with a slightly lower activity and selectivity to DMM (at 423 K, VTiS-CP: conversion = 61%, S_{DMM} = 86%, vs. VTiS-CPEG: conversion = 28%, S_{DMM} = 56%). This can be attributed to a decreased reducibility and surface acidity upon addition of 1 wt% PEG-400. For samples prepared by sol–gel and mechanical grinding, a different behavior was observed. In fact, even increasing the reaction temperature up to 443 K, no formic acid (FA) production could be observed, and a very high selectivity towards DMM (72 and 84% respectively for VTIS-SG and VTIS-MG) was maintained. These results can be related to the higher percentage of SO_4^{2-} present on these two samples, which can both inhibit the activity of the redox sites (connected to FA production) and/or prevent the deactivation of the acidic sites even at high reaction temperature [4].

Furthermore, the selectivity to DME (usually created on strong acid sites) over the VTiS-MG catalyst prepared by mechanical grinding was higher and increased with increasing reaction temperatures. Of all catalysts studied in this work, the VTiS-CP sample was found to be the most effective in the selective oxidation of methanol to DMM with 61% conversion of methanol and 86% selectivity to DMM, probably due to the presence of the highest amount of vanadia surface species and an appropriate content of SO_4^{2-}.

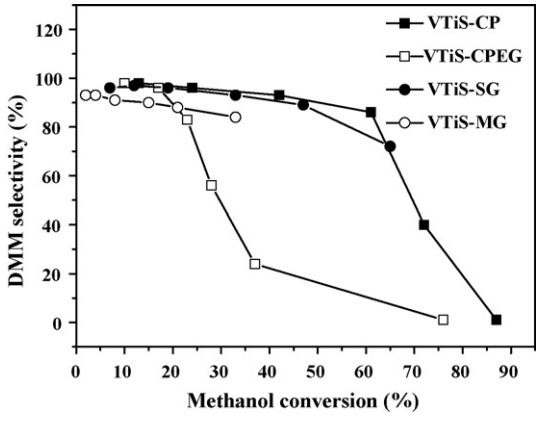

Fig. 7. DMM selectivity vs. methanol conversion over VTiS catalysts.

4. Conclusion

As expected, the surface and catalytic properties of V_2O_5–TiO_2/SO_4^{2-} catalysts were greatly influenced by different preparation methods. Crystallites of V_2O_5 were detected for all samples by Raman spectroscopy. Moreover, Raman spectroscopy also suggested that the sample prepared by mechanical grinding was not homogeneous. The ammonia adsorption calorimetric study showed the special behavior of NH_3 dissociation at the surface of some samples, those containing a high content of sulfur. However, pyridine adsorption FT-IR did not show an obvious difference of surface acidity between the samples, and indicated the coexistence of both Lewis and Brønsted acid sites for all VTiS catalysts studied in this work. The co-precipitated catalyst VTiS-CP was found to exhibit the best performance for the selective oxidation of methanol to DMM. Specifically, the conversion of methanol could be as high as 61% over VTiS-CP, with a high DMM selectivity of 86% at 423 K. Meanwhile, catalytic methanol oxidation was also successfully used to investigate the quantities of surface active sites. In conclusion, the acidic and catalytic properties were affected on one hand by the preparation method and on the other hand by the SO_4^{2-} content.

Acknowledgements

The authors are thankful to the scientific services of IRCELYON and in particular to P. Mascunan, for providing O_2 chemisorption and Raman measurements.

Hongying Zhao gratefully acknowledges the China Scholarship Council for the financial support of her PhD grant. Financial

supports from NSFC (20673055), MSTC (2005CB221400 and 2004DFB02900) and Jiangsu Province, China (BG2006031) are acknowledged.

References

[1] F. Roozeboom, P.D. Cordingley, P.J. Gellings, J. Catal. 68 (1981) 464–472.
[2] P. Forzatti, E. Tronconi, G. Busca, P. Tittarelli, Catal. Today 1 (1987) 209–218.
[3] A. Baiker, D. Monti, J. Catal. 91 (1985) 361–365.
[4] S. Royer, X. Sécordel, M. Brandhorst, F. Dumeignil, S. Cristol, C. Dujardin, M. Capron, E. Payen, J.-L. Dubois, Chem. Commun. 7 (2008) 865–867.
[5] Y. Fu, J. Shen, Chem. Commun. 21 (2007) 2172–2174.
[6] S. Damyanova, M.L. Cubeiro, J.L.G. Fierro, J. Mol. Catal. A: Chem. 142 (1999) 85–100.
[7] C.R. Anthony, L. Mcelwee-White, J. Mol. Catal. A: Chem. 227 (2005) 113–117.
[8] K. Fuji, S. Nakano, E. Fujita, Synthesis 4 (1975) 276–277.
[9] J. Masamoto, T. Iwaisako, M. Chohno, M. Kawamura, J. Ohtake, K. Matsuzaki, J. Appl. Polym. Sci. 50 (1993) 1299–1305.
[10] Q. Sun, A. Auroux, J. Shen, J. Catal. 244 (2006) 1–9.
[11] S. Satoh, Y. Tanigawa, US Patent 6,379,507 (2002).
[12] J.M. Tatibouët, Appl. Catal. A 148 (1997) 213–252.
[13] M. Badlani, I.E. Wachs, Catal. Lett. 75 (2001) 137–149.
[14] L.E. Briand, Met. Oxides: Chem. Appl. 108 (2006) 353–390.
[15] A. Auroux, Top. Catal. 4 (1997) 71–89.
[16] F. Belkhadem, J.-M. Clacens, A. Bengueddach, F. Figueras, Appl. Catal. A 298 (2006) 188–193.
[17] H. Zhao, S. Bennici, J. Shen, A. Auroux, Appl. Catal. A 356 (2009) 121–128.
[18] S.T. Oyama, G.T. Went, K.B. Lewis, A.T. Bell, G.A. Somorjai, J. Phys. Chem. 93 (1989) 6786–6790.
[19] B.S. Parekh, S.W. Weller, J. Catal. 47 (1977) 100–108.
[20] S.W. Weller, Acc. Chem. Res. 16 (1983) 101–106.
[21] B.M. Reddy, B. Manohar, E.P. Reddy, Langmuir 9 (1993) 1781–1785.
[22] I.E. Wachs, Catal. Today 27 (1996) 437–455.
[23] G.T. Went, L.J. Leu, A.T. Bell, J. Catal. 134 (1992) 479–491.
[24] M.D. Amiridis, I.E. Wachs, G. Deo, J.M. Jehng, D.S. Kim, J. Catal. 161 (1996) 247–253.
[25] G.T. Went, L.J. Leu, R.R. Rosin, A.T. Bell, J. Catal. 134 (1992) 492–505.
[26] I.R. Beattie, T.R. Gilson, J. Chem. Soc. A (1969) 2322–2327.
[27] F. Roozeboom, M.C. Mittelmeijer-Hazeleger, J.A. Moulijn, J. Medema, V.H.J. De Beer, P.J. Gellings, J. Phys. Chem. 84 (1980) 2783–2791.
[28] J.P. Dunn, J.M. Jehng, D.S. Kim, L.E. Briand, H.G. Stenger, I.E. Wachs, J. Phys. Chem. B 102 (1998) 6212–6218.
[29] J. Keränen, A. Auroux, S. Ek-Härkönen, L. Niinistö, Thermochim. Acta 379 (2001) 233–239.
[30] K. Tanabe, Mater. Chem. Phys. 17 (1987) 217–225.
[31] A. Desmartin-Chomel, J.L. Flores, A. Bourane, J.-M. Clacens, F. Figueras, G. Delahay, A. Giroir Fendler, C. Lehaut-Burnouf, J. Phys. Chem. B 110 (2006) 858–863.
[32] A. Gervasini, J. Fenyvesi, A. Auroux, Langmuir 12 (1996) 5356–5364.
[33] A. Gervasini, A. Auroux, J. Phys. Chem. 97 (1993) 2628–2639.
[34] F. Hatayama, T. Ohno, T. Maruoka, T. Ono, H. Miyata, J. Chem. Soc., Faraday Trans. 87 (1991) 2629–2633.
[35] T. Blasco, A. Galli, J.M. López Nieto, F. Trifiró, J. Catal. 169 (1997) 203–211.
[36] J. Keränen, A. Auroux, S. Ek, L. Niinistö, Appl. Catal. A 228 (2002) 213–225.
[37] J. Datka, A.M. Turek, J.M. Jehng, I.E. Wachs, J. Catal. 135 (1992) 186–199.
[38] Q. Sun, Y. Fu, J. Liu, A. Auroux, J. Shen, Appl. Catal. A 334 (2008) 26–34.
[39] M. Amiridis, R. Duevel, I. Wachs, Appl. Catal. B 20 (1999) 111–122.
[40] T. Barzetti, E. Selli, D. Moscotti, L. Forni, J. Chem. Soc., Faraday Trans. 92 (1996) 1401–1407.
[41] H. Miyata, K. Fujii, S. Inui, Y. Kubokawa, Appl. Spectrosc. 40 (1986) 1177–1180.
[42] H. Miyata, Y. Nakagawa, S. Miyagawa, Y. Kubokawa, J. Chem. Soc., Faraday Trans. 1 (84) (1988) 2129–2134.